Hydrogenated Amorphous Silicon High Flux X-ray Detectors for Synchrotron Beam Monitoring Applications

M.J. Large[1,*], M.Bizzarri[2,3], M.Boscardin[4,5], L.Calcagnile[6], M. Caprai[2], A.P. Caricato[6], G.A.P. Cirrone[7], M. Crivellari[5], I. Cupparo[8], G. Cuttone[7], S.Dunand[9], L. Fanò[2,3], B.Gianfelici[2,3], O. Hammad[5], M. Ionica[2], K. Kanxheri[2], G. Maruccio[6], M. Menichelli[2], A. Monteduro[6], F. Moscatelli[2,10], A. Morozzi[2], A. Papi[2], D. Passeri[2,11], M.Pedio[2,10], F.Peverini[2,3], G.Quarta[6], S. Rizzato[6] , A. Rossi[2,3], G. Rossi[2], A. Scorzoni[2,11], L. Servoli[2], C. Talamonti[8], G. Verzellesi[4,12], N. Wyrsch[9] & M. Petasecca[1]

***Abstract*—A series of radiation hard a-Si:H diodes have been characterized for X-ray dosimetry and real-time beam monitoring applications in extremely high flux beamlines such as those pertaining to synchrotron facilities. These devices displayed superior radiation hardness under constant high dose-rate irradiations of 1010 kGy/s, with a variation in response of with 10% over a delivered dose range of ~800 kGy. The sensitivities and dose linearity of each detector to X-rays with a peak energy of 117 keV is reported, with sensitivities ranging from (2.74±0.02) nC/Gy to (4.96±0.02) nC/Gy. For detectors with 0.8 µm thick active a-Si:H layer, their operation in an edge-on orientation allowed for the reconstruction of micron-size beam profiles (Microbeams). The microbeams, with a nominal full-width-half-max of 50 µm and a peak-to-peak separation of 400 µm, were reconstructed with extreme accuracy, with their full-width-half-max observed as 55.4 ± 0.5 µm with detectors placed in water equivalent plastic at a depth of 15 mm. An XBIC charge collection map of a single 4x4 mm^2 pixel of the a-Si:H diodes is also presented.**

***Index Terms*—Radiation damage; synchrotron radiation; Microbeam; hydrogenated amorphous silicon; high dose-rate**

I. INTRODUCTION

THIS work presents a study in the use of hydrogenated amorphous silicon planar diode structures employed as radiation hard X-ray detectors for dosimetry and beam monitoring of high intensity synchrotron X-ray microbeams. X-ray microbeams are adopted in advanced radiotherapy modalities such as Microbeam Radiotherapy and photon-FLASH therapy. There is an extensive effort in the medical physics community in exploring new materials for dosimetry of such radiotherapy modalities due to the limitations of standard dosimetric devices adopted in modern radiotherapy.

The generation of ultra-high dose-rate X-rays at synchrotron facilities is extremely attractive as an improved radiotherapy treatment modality. Known as the "FLASH" effect, the exposure of tumor tissue to dose rates on the order of 10 kGy/s has been reported to result in lessened damage to surrounding normal tissues whilst maintaining tumor control similar to that seen in conventional radiotherapy techniques delivering 6 Gy/min [1, 2]. Additionally, the collimation of high dose-rate synchrotron beams into multiple micron-sized beams (known as Microbeam Radiation Therapy, MRT) has demonstrated promising results in animal-based studies with improved sparing of surrounding normal tissues [3]. As the development of MRT moves towards clinical applications, devices that can accurately monitor dose deposited during treatment and resolve the profile of microbeams with high spatial resolution are vital.

Intrinsic a-Si:H device layers are produced via Plasma Enhanced Chemical Vapor Deposition (PECVD) of a mixture of Silane gas (SiH_4) and molecular hydrogen at temperatures of up to 300^{o}C. PECVD allows for the deposition of a-Si:H over large areas at low cost with high reproducibility. Furthermore, PECVD allows for the fabrication of a-Si:H devices on a wide variety of substrates including flexible substrates such as polyamide (Kapton ©), polyethylene naphthalate (PEN) and polyethylene terephthalate (PET). The resulting material is a disordered semiconductor with short-range order. In a-Si, the absence of long-range order gives rise to rise to broken or unsatisfied Si-Si bonds resulting in tail states from both the

This work was partially supported by the "Fondazione Cassa di Risparmio di Perugia" RISAI project n. 2019.0245.
1. Centre for Medical Radiation Physics, University of Wollongong, Northfields Ave Wollongong NSW 2522, (AUSTRALIA).
2. INFN, Sez. di Perugia, via Pascoli s.n.c. 06123 Perugia (ITALY).
3. Dip. di Fisica e Geologia dell'Università degli Studi di Perugia, via Pascoli s.n.c. 06123 Perugia (ITALY).
4. INFN, TIPFA Via Sommarive 14, 38123 Povo (TN) (ITALY).
5. Fondazione Bruno Kessler, Via Sommarive 18, 38123 Povo (TN) (ITALY).
6. INFN and Dipartimento di Fisica e Matematica dell'Università di Lecce, Via per Arnesano, 73100 Lecce (ITALY).
7. INFN Laboratori Nazionali del Sud, Via S.Sofia 62, 95123 Catania (ITALY).
8.INFN and Dipartimento di Fisica e Astronomia dell'Università di Firenze, Via Sansone 1, 50019 Sesto Fiorentino (FI) (ITALY).
9. Ecole Polytechnique Fédérale de Lausanne (EPFL), Institute of Microengineering (IMT), Rue de la Maladière 71b, 2000 Neuchâtel, (SWITZERLAND).
10. CNR-IOM, via Pascoli s.n.c. 06123 Perugia (ITALY).
11. Dip. di Ingegneria dell'Università degli studi di Perugia, via G.Duranti 06125 Perugia (ITALY).
12. Dip. di Scienze e Metodi dell'Ingegneria, Università di Modena e Reggio Emilia, Via Amendola 2, 42122 Reggio Emilia (ITALY).
* Corresponding author, mjl970@uowmail.edu.au

conduction and valence bands which extend into the band gap [4]. For a-Si:H, the introduction of hydrogen (at least 4 - 10 % atomic) passivates the effect of most of the dangling bonds, reducing defects within the amorphous silicon structure and improving the ability of the material to conduct electricity and to allow doping to be possible [5].

An advantageous feature of a-Si:H is its superior radiation hardness, with Wyrsch *et al.* reporting an increase in the leakage current of a 32.6 µm a-Si:H p-i-n diode of only a factor of 2 when held at a 9×10^4 V/cm electric field and irradiated with 24 GeV protons up to a fluence of 7×10^{15} p/cm^2 [6]. Detailed motivations behind the use of a-Si:H diodes for beam monitoring and dosimetry in high-dose environments is presented in full in (Menichelli *et al.*, 2020) [7]. In this work, we characterize the response of a set of a-Si:H planar diodes to high dose-rate broad beam and microbeam synchrotron radiation.

II. Materials and Methods

The a-Si:H detectors were fabricated by EPFL (Lucerne, Switzerland) and consist of electron selective contacts of ZnO:Al or TiO_2 deposited on glass with thicknesses of 60 nm or 10 nm, respectively. The active a-Si:H detector layer is deposited via PECVD at thicknesses of 0.8 µm and 6.2 µm. Device top contacts were fabricated with a 20 nm thick MoO_x layer protected by 60 nm of indium titanium oxide (ITO). Each device contains 4 pixels with an area of 4x4 mm^2. The devices are mounted on Kapton PCB tails and readout in real time using a custom designed electrometer developed by the Centre for Medical Radiation Physics (CMRP) at the University of Wollongong, Australia. Pixels of the a-Si:H devices are connected to the Kapton PCB tails via thin copper wires bonded with silver paint and epoxy to the top contact. The geometry of the detectors are depicted in figure 1.

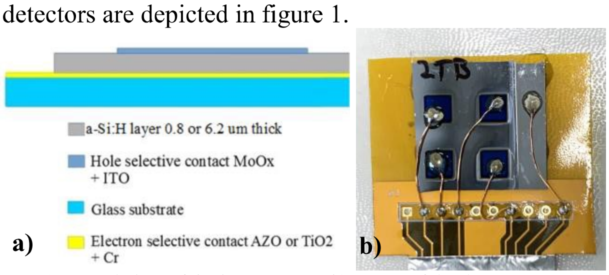

Fig. 1. a) Lateral view of device structure. b) Image of the detector on Kapton tail from above. Pixels are 4x4 mm^2 in area.

Measurements were performed at the Australian Synchrotron (AS) on the Imaging and Medical Beamline (IMBL). A wiggler field of 4T was applied to the electron beam to produce synchrotron radiation. The beam height was controlled through the use of beam-defining apertures (BDAs) with 2, 1 or 0.5 mm heights. Beam width and overall field-size were defined by a 20x20 mm^2 conformal tungsten mask. The delivered dose-rate and average energy of the beam were modulated through the use of beam filters composed of aluminium (Al), copper (Cu) or molybdenum (Mo), with further details provided in Table I.

Table I. Beam properties as measured with PTW Type 31022 PinPoint chamber exposed to 4T "pink" beam with 2mm BDA and 20x20 mm^2 field (measured at 10mm/s scan speed).

Beam Filtration	Peak Energy (keV)*	Dose Rate @15mm depth (Gy/s)	Dose Rate @37mm depth (Gy/s)
Al-Al	47.8	6963	5041
Cu-Cu	87.5	700	523
Mo-Mo$^+$	117	128	93

*Peak energies from Livingstone *et al.*(2018) [8].
$^+$Short-hand for AlMo-AlMo filtration.

A. Radiation Damage

The effects of radiation damage were investigated on 6.2 µm thick a-Si:H detectors exposed to a total ionizing dose upwards of 1000 kGy in steps of 20-100 kGy. Such large doses were delivered using the 4T Al-Al "pink" beam modality of the IMBL in broad beam conditions, producing the highest dose rate available at the IMBL. Devices were placed at a 15mm depth in solid water and subject to multiple 10mm/s vertical scans with the beam height set via BDA at 2mm and scanned over the 20x20 mm^2 field to deliver ~1400 Gy per scan. Devices were held at a 3V reverse bias during irradiations. After each irradiation step, the response of the a-Si:H detectors at 3V reverse bias to three 10mm/s vertical scans with Mo-Mo filtration (lowest dose rate) were recorded, measuring integral response and fluctuation of the baseline as a function of total ionizing dose.

B. Dose Linearity

The response of all 4 a-Si:H devices (0.8 µm and 6.2 µm thicknesses, ZnO:Al and TiO_2 electron selective contacts) operated in photovoltaic mode (0V bias) were recorded. The devices were exposed to a 4T Mo-Mo beam with 2mm BDA and 20x20 mm^2 field size at a depth of 37mm in solid water. The device was scanned vertically through the beam at speeds of 5, 10 and 20 mm/s, delivering a dose of 40, 20 and 10 Gy/scan respectively. At each scan speed, 3 repetitions were performed with the response recorded as the average over the 3 scans and uncertainty represented as the standard deviation.

C. Microbeam Profile Characterization

To spatially fractionate the synchrotrons 4T Mo-Mo broad beam, a tungsten multi-slit collimator (MSC) was placed in the beam resulting in the creation of 50 microbeams with 50 µm Full-Width-Half-Max (FWHM) and a peak-to-peak pitch of 400 µm. A filtering choice of the 4T-MoMo spectrum in this modality was selected in order to be coherent with the reference dosimetry. The 0.8 µm thick a-Si:H diode with ZnO:Al electron selective contact was situated edge-on (device surface parallel to beam) and scanned laterally across the microbeams at a speed of 2 mm/s. Using CMRPs custom designed electrometer with a 0.16 ms signal integration time, the profile of all 50 microbeams was reconstructed with a spatial resolution of 320 nm.

D. X-ray Beam Induced Charge (XBIC) Mapping

With the MSC placed in the beam operated at 4T wiggler field and with Cu-Cu filtration, the beam was further confined such that only a single microbeam with dimensions 500 µm x 50 µm was incident on the 6.2 µm ZnO:Al detector. The detector was held at 10V reverse bias and irradiated at surface conditions

(0mm depth). The single microbeam was scanned laterally across a single 4x4 mm^2 pixel of the detector. Each scan moved through an 8mm range and was repeated at various heights in 0.5 mm steps, with the induced charge collected at the pixel recorded as a function of beam position. The resulting data was used to produce a 2D charge collection map of the chosen pixel.

III. Results

The radiation resistance of the 6.2 µm sample with ZnO:Al electron selective contact at a depth of 37mm in water equivalent material is presented in figure 2. In figure 2a, the integral charge collected in a single pixel of the device (see fig. 1) from a 10mm/s scan over a 20x20 mm^2 field of the 4T-MoMo "pink" broad beam (2mm BDA) is presented as a function of total ionizing dose (TID). Following an initial decrease in response by 55% between 0-115kGy, the device exhibited an extremely stable response over a large TID range of 115-1000 kGy, displaying the superior radiation hardness of a-Si:H with the device's response varying by ±10%. In figure 2b, we observe a linearly increasing leakage current with increasing TID. However, two drops in leakage current from point 1 to 2 and 3 to 4. These decreases correspond to time periods of 30 and 60 minutes where the device was not irradiated and instead allowed to anneal at room temperature.

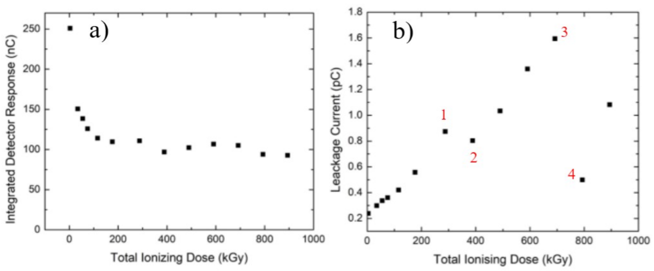

Fig. 2. a) Integral charge as a function of total ionizing dose delivered to pixel 3 of the 6.2 µm thick a-Si:H diode with ZnO:Al electron selective contact at a depth of 37 mm in water equivalent material and held at a 3V reverse bias. b) Variation of the devices leakage current as a function of total ionizing dose.

The linearity of response with delivered dose was investigated in 4 devices operated in photovoltaic mode (0V bias) – the 4 devices being unique combinations of active layer thickness (0.8 µm or 6.2 µm) and electron selective contact (ZnO:Al or TiO_2). Figure 3 displays the linearity's of these 4 devices as measured via exposure to the 4T-MoMo modality of the synchrotron broad beam. Table 2 presents the resulting device sensitivities calculated from the gradient of the data series in fig. 2.

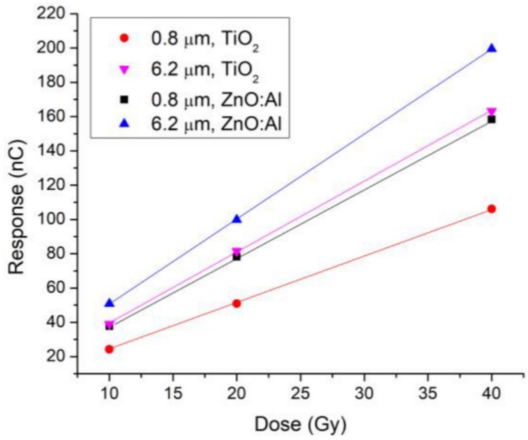

Fig 3. Linear response of a-Si:H diodes as a function of delivered dose. Devices were placed at a 37 mm depth in water equivalent material and exposed to 4T-MoMo broad beam modality of the synchrotron beam shaped with a 2 mm BDA and 20x20 mm^2 field.

Table II. Device sensitivities as calculated from the gradients of the results in fig. 3.

Thickness (µm)	Contact Material	Sensitivity (nC/Gy)
0.8	ZnO:Al	4.02 ± 0.01
	TiO_2	2.74 ± 0.02
6.2	ZnO:Al	4.96 ± 0.02
	TiO_2	4.13 ± 0.04

With the thinnest device (0.8 µm, ZnO:Al electron selective contact) oriented edge-on with respect to the collimated 4T-CuCu beam, the profile of the IMBL's synchrotron microbeams was reconstructed in high resolution and with extreme accuracy. The measured FWHM of the microbeams displayed in figure 4 was calculated as (55.4 ± 0.5) µm. In comparison, the nominal width of the measured microbeams have an expected FWHM of 50 µm. This result demonstrates the impressive spatial resolution with which the a-Si:H detectors can operate.

A charge collection efficiency map was created using XBIC techniques as discussed in the methods section. The resulting map of a single pixel of the 6.2 µm thick device with ZnO:Al electron selective contact is depicted in figure 5. In the figure, the outline of the 4x4 mm2 pixel area is visible at a level just above the background noise. As we move towards the center of the pixel a number of interesting features appear. The lighter-blue region in the center that extends to the top left of the image is dose enhancement caused by the epoxy resin used to bond the wire contact in place. Furthermore, the region of highest charge collection in the very center is again due to dose enhancement localized to this region, but here due to the silver paste used for wire bonding. A side-by-side comparison is made between an image of the pixel in fig 5b and the XBIC charge map of fig 5a.

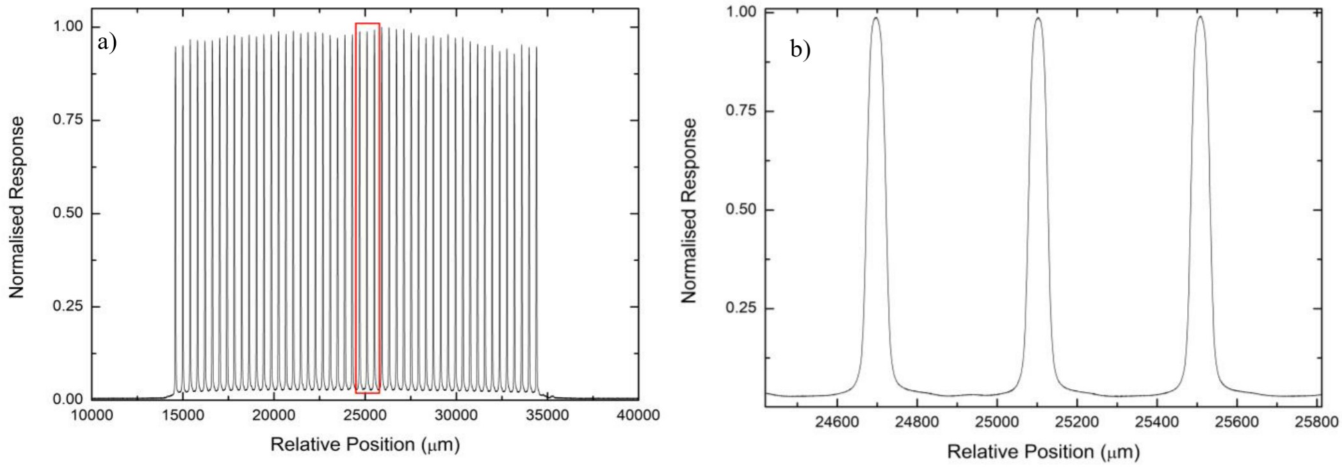

Fig. 4. a) Intrinsic microbeam profile scan of 4T-CuCu synchrotron broad beam collimated into 50 micron-sized beams, as re-constructed by 0.8 μm thick a-Si:H diode in edge-on modality and scanned laterally through the field 20x20 mm2 field (0.5 mm BDA) at 2 mm/s. b) High-resolution re-construction of 3 central microbeams (encased in red area of fig 4a).

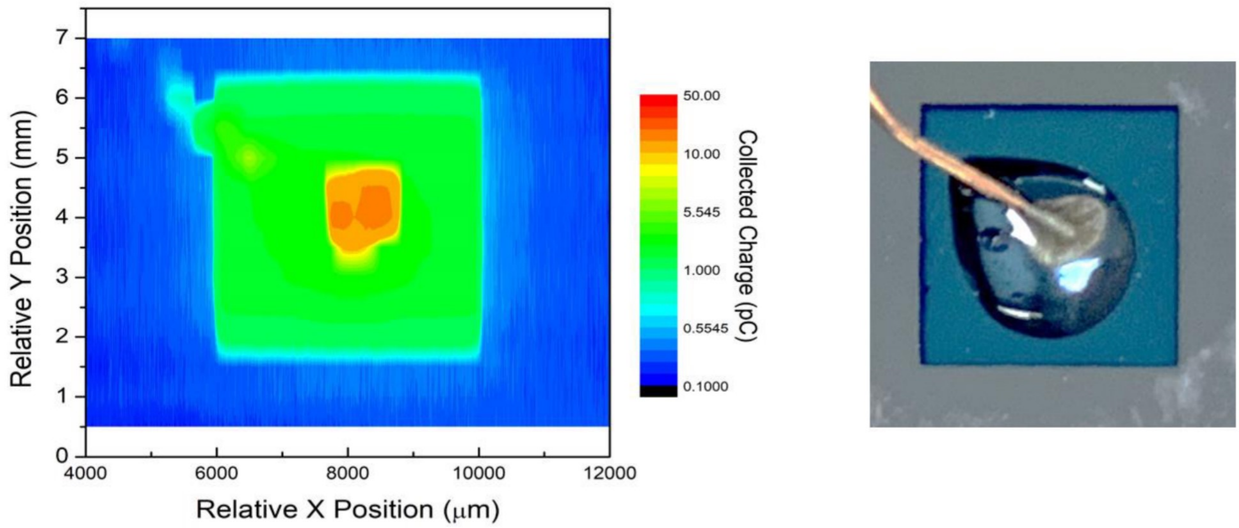

Fig. 5. a) X-ray beam induced charge map of pixel 3 of the 6.2 μm thick a-Si:H diode with ZnO:Al electron selective contact. Device was held at a 10V reverse bias during charge collection mapping. Mapped using a single microbeam (4T-CuCu modality) traversing the pixel in a series of lateral scans at 1 mm/s. b) Image of the pixel mapped via XBIC methods.

IV. Conclusion

The results presented in this summary demonstrate the feasibility of a-Si:H diodes for applications in X-ray dosimetry and beam monitoring in high dose-rate environments, such as those in FLASH radiotherapy and Microbeam Radiation Therapy treatments. The devices tested have displayed superior radiation hardness, excellent spatial resolution and an extremely linear response to variations in delivered dose. An in-depth analysis of these results accompanied by further results will be presented in full at the RADECS 2022 conference.

References

[1] J. A. Posar, M. J. Large, S. Alnaghy *et al.* (2021, Sept.), Towards high spatial resolution tissue-equivalent dosimetry for microbeam radiation therapy using organic semiconductors. *J. Synch. Rad. 28(5),* pp. 1444 – 1454.

[2] J. D. Wilson, E. M. Hammond, G. S. Higgins & K. Petersson (2020, Jan.), Ultra-High Dose Rate (FLASH) Radiotherapy: Silver Bullet or Fool's Gold? *Front. Oncol. 9*, pp. 1–12.

[3] E. Engels, N. Li, J. Davis *et al*. (2020), Toward personalized synchrotron microbeam radiation therapy. *Sci. Rep. 10* [online], https://doi.org/10.1038/s41598-020-65729-z.

[4] A. Klaver, "Irradiation-induced degradation of amorphous silicon solar cells in space," Phd thesis, Delft University of Technology, 2007.

[5] R. A. Street. (1991). Hydrogenated Amorphous Silicon. *Cambridge Solid State Science Series*.

[6] N. Wyrsch *et al.* (2006), Radiation hardness of amorphous silicon particle sensors, *J. Non-Cryst. Solids 352,* 1797.

[7] M. Menichelli *et al.* (2020), Hydrogenated amorphous silicon detectors for particle detection, beam flux monitoring and dosimetry in high-dose radiation environment, *J. Inst (15), C04005* [online], https://iopscience.iop.org/article/10.1088/1748-0221/15/04/C04005.

[8] J. Livingstone *et al*. (2018), Experimental optimisation of the X-ray energy in microbeam radiation therapy, *Phys Med 45*, pp. 156-161.